

Enhanced moments of inertia for rotation in neutron-rich nuclei

Kenichi Yoshida^{1,*}

¹*Department of Physics, Kyoto University, Kyoto, 606-8502, Japan*

(Dated: May 5, 2022)

Ground-state moments of inertia (MoI) are investigated for about 1700 even-even nuclei from the proton drip line to the neutron drip line up to $Z = 120$ and $N = 184$. The cranked Skyrme–Hartree–Fock–Bogoliubov equation is solved in the coordinate space. This model describes well the available experimental data of more than 300 nuclides possessing an appreciable deformation. I find that the MoI greatly increase near the drip line whereas the deformation is not as strong as estimated by the empirical relation. Systematic measurements of the excitation energy and the transition probability to the first $I^\pi = 2^+$ state in neutron-rich nuclei not only reveal the evolution of deformation but can also constrain an effective pair interaction.

I. INTRODUCTION

Nuclear rotational motion emerges due to the spontaneous breaking of the rotational symmetry [1]. As stepping away from the magic number, the first $I^\pi = 2^+$ state becomes lower in energy: The collective mode of excitation changes its character from the vibration to the rotation as the deformation develops. A naïve question arises here: How strong should the deformation be for the picture of the rotation to be well-drawn?

Recently, various spectroscopic studies have been carried out to explore unique structures in neutron-rich nuclei. The excitation energy of the 2_1^+ state, $E(2_1^+)$, is often among the first quantities accessible in experiments and systematic measurements have revealed the evolution of the shell structure [2–4]. Besides the change of the shell structure associated with the onset of deformation, the $E(2_1^+)$ value may provide rich information on exotic nuclei. A significant lowering of $E(2_1^+)$ observed in a near-drip-line nucleus ^{40}Mg could be a signal of new physics in drip-line nuclei [5], as the theoretical calculations have predicted that the magnitude of deformation is not enhanced in ^{40}Mg comparing with the Mg isotopes with less neutrons [6–13].

The pair correlation is present in the ground state and plays a decisive role in describing various phenomena such as the energy gap in spectra of even-even nuclei, the odd-even staggering in binding energies and so on [14, 15]. Furthermore, the pairing is indispensable for a strong collectivity of the low-frequency quadrupole vibration [16] and a reduced value of moments of inertia (MoI) for rotation from the rigid-body estimation [14]. Therefore, the $E(2_1^+)$ value should be scrutinized by taking not only the deformation but the superfluidity into account.

Another critical issue in exploring the drip-line nuclei is a need of the careful treatment of the asymptotic part of the nucleonic density. An appropriate framework is Hartree–Fock–Bogoliubov (HFB) theory, solved in the coordinate-space representation [17, 18]. This method

has been used extensively in the description of spherical systems but is much more difficult to implement for systems with deformed equilibrium shapes. Therefore, calculations have been mostly restricted to axially symmetric nuclei [19–24]. A standard technique to describe the non-axial shapes is to employ a truncated single-particle basis, which consists of localized states and discretized-continuum oscillating states, for solutions of the HFB equation [25]. Such a method should not be able to describe adequately the spatial profile of densities at large distances. Recently, the HFB equation has been solved by employing the contour integral technique and the shifted Krylov subspace method for the Green’s function [26, 27] to circumvent the successive diagonalization of the matrix with huge dimension.

In this work, I investigate the rotational motion in neutron-rich nuclei near the drip line with emphasizing the pairing. At high spins where the pairing vanishes, proposed is a novel mechanism of a nucleus being bound beyond the neutron drip line [28]. Here, I study the lowest spin state, namely the 2_1^+ state, in even-even non-spherical nuclei. A key quantity is the MoI for rotation: $E(2_1^+) = 6/2\mathcal{J}$.

II. MODEL AND METHOD

The MoI is evaluated microscopically by the Thouless–Valatin procedure or the self-consistent cranking model as $\mathcal{J} = \lim_{\omega_{\text{rot}} \rightarrow 0} \frac{J_x}{\omega_{\text{rot}}}$ with $J_x = \langle \hat{J}_x \rangle$ and ω_{rot} being the rotational frequency about the x -axis [14]. I solve the cranked HFB (CHFB) equation to obtain the MoI and take the natural units: $\hbar = c = 1$.

The numerical procedure to solve the CHFB equation is described in Ref. [29]: I impose the reflection symmetry about the (x, y) -, (y, z) - and (z, x) -planes. Thus, the parity \mathbf{p}_k ($= \pm 1$) and x -signature r_k ($= \pm i$) are a good quantum number. I solve the CHFB equation by diagonalizing the HFB Hamiltonian in the three-dimensional (3D) Cartesian-mesh representation with the box boundary condition. Thanks to the reflection symmetries, I have only to consider the octant region explicitly in space with $x \geq 0$, $y \geq 0$, and $z \geq 0$; see Refs. [30, 31] for

* E-mail: kyoshida@ruby.scphys.kyoto-u.ac.jp

details. I use a 3D lattice mesh $x_i = ih - h/2, y_j = jh - h/2, z_k = kh - h/2$ ($i, j, k = 1, 2, \dots, M$) with a mesh size $h = 1.0$ fm and $M = 12$ for each direction. A reasonable convergence with respect to the mesh size h and the box size M is obtained for not only drip-line nuclei but medium-mass nuclei [29]. For diagonalizing the HFB matrix, I use the ScaLAPACK PDSYEV subroutine [32]. A modified Broyden's method [33] is utilized to calculate new densities during the self-consistent iteration. The quasiparticle energy is cut off at 60 MeV. For each iteration, it takes about 10 core hours at the SQUID computer facility (composed of 1520 nodes of Intel Xeon Platinum 8368 processor) of Osaka University. To obtain the convergence, typically, 50–100 iterations are needed. Therefore, the total cost for a systematic calculation of 1700 nuclei is about 17000 node hours.

III. RESULTS AND DISCUSSION

A. Validity of the present model

The MoI of the ground state is evaluated at $\omega_{\text{rot}} = 0.05$ MeV. I employed the SkM* [34] and SLy4 [35] functionals augmented by the Yamagami–Shimizu–Nakatsukasa (YSN) pairing-density functional [36], which is given as

$$\mathcal{E}_{\text{pair}}(\mathbf{r}) = \frac{V_0}{4} \sum_{\tau=\text{n,p}} g_{\tau}[\rho, \rho_1] |\tilde{\rho}_{\tau}(\mathbf{r})|^2 \quad (1)$$

with

$$g_{\tau}[\rho, \rho_1] = 1 - \eta_0 \frac{\rho(\mathbf{r})}{\rho_0} - \eta_1 \frac{\tau_3 \rho_1(\mathbf{r})}{\rho_0} - \eta_2 \left[\frac{\rho_1(\mathbf{r})}{\rho_0} \right]^2. \quad (2)$$

Here, $\rho(\mathbf{r})$ and $\rho_1(\mathbf{r})$ are the isoscalar and isovector densities, $\tau = \text{n}$ (neutron) or p (proton), and $\rho_0 = 0.16$ fm $^{-3}$ is the saturation density of symmetric nuclear matter. The parameters $V_0, \eta_0, \eta_1, \eta_2$ were optimized to reproduce the experimental pairing gaps globally and are summarized in Table III of Ref. [36]. Note that the parameters for the ρ_1 dependence η_1, η_2 are positive. The YSN pairing functional was constructed based on the finding that the inclusion of the isospin dependence in the pairing functional gives a good reproduction of the pairing gaps in both stable and neutron-rich nuclei and in both symmetric nuclear matter and in neutron matter [37, 38].

There are 657 even-even nuclei with known $E(2_1^+)$ [39]. In the present study here I limit the scope by excluding the very light nuclei ($Z < 10$), for which mean-field theory is least justified. This eliminates 22 nuclei. The experimental data evaluated as $3/E(2_1^+)$ for 635 nuclei are displayed in Fig. 1(e). There is no collective rotation in spherical nuclei where the MoI is zero. Actually, I defined the spherical nuclei if the calculated MoI is less than 0.1 MeV $^{-1}$. An additional 273 (260) nuclei have been eliminated for that reason, leaving 362 (375) nuclei in the present analysis.

Figures 2(a) and 2(b) show the calculated MoI obtained by using SkM* and SLy4 versus experimental ones. The points follow the diagonal line reasonably well with some scatters that vary in extent over the different regimes. For transitional nuclei, one may wonder about the validity of the present model. The filled symbols in Figs. 2(a) and 2(b) denote the weakly deformed nuclei having $\beta < 0.1$. These nuclei give a small value for the MoI, corresponding to higher $E(2_1^+)$ than measurement. Furthermore, one sees a distinct deviation from the straight line for the highest region around $\mathcal{J} = 60$ MeV $^{-1}$: $^{238,240}\text{Cm}$ and ^{244}Cf .

To make a quantitative measure of the theoretical accuracy, I compare theory and experiment, and examine the statistical properties of the quantity $R = \mathcal{J}_{\text{th}}/\mathcal{J}_{\text{exp}}$. Here \mathcal{J}_{th} and \mathcal{J}_{exp} are the theoretical and experimental MoI. A histogram of the distribution of R is shown in Figs. 2(c) and 2(d). For SkM* (SLy4), the average is $\bar{R} = 1.02$ (1.16). When excluding the weakly deformed nuclei with $\beta < 0.1$, $\bar{R} = 1.07$ (1.15) for 332 (350) data. Therefore, the present model overestimates the MoI by about 10%.

The width of the distribution is an important quantity to determine the accuracy and reliability of the theory. One sees that the error is systematic, and the overall distribution is strongly peaked when excluding the weakly deformed nuclei that cause a tail in small R . The root-mean-square deviation, the dispersion, of R about its mean is $\sigma = 0.09$ (0.12). Thus, a typical error is about 10%.

It is interesting to compare the present calculation with the beyond-mean-field type calculations [40, 41]. The excited 2^+ states were obtained by the minimization after projection (MAP) and the generator coordinate method (GCM) using the SLy4 functional [40] or the 5-dimensional collective Hamiltonian (5DCH) based on the GCM together with the Gaussian overlap approximation using the Gogny D1S functional [41]. The authors in Refs. [40, 41] introduced the measure $R_E = \ln(E_{\text{th}}(2^+)/E_{\text{exp}}(2^+))$ to evaluate the validity of the theoretical framework. Then, I evaluate $E(2^+)$ as $3/\mathcal{J}$ in the present model.

Table I summarizes the statistics for the performance. The present model gives a compatible description for the average of the energy to the 5DCH approach for deformed nuclei. The dispersion is better than in other models. This comparison indicates that the 2_1^+ state is mostly governed by the rotational MoI of the ground state, and the self-consistent cranking model describes the 2_1^+ state surprisingly well for deformed nuclei with $\beta > 0.1$. However, it does not mean the rotational band with the excitation energy $\propto I(I+1)$ always appears in deformed nuclei with $\beta > 0.1$ because the MoI in the cranking model depends on spins.

I briefly mention the performance for the intrinsic quadrupole deformation. For selected nuclei of the Nd and Sm isotopes, it was demonstrated that the mean-field approximation describes well the evolution of de-

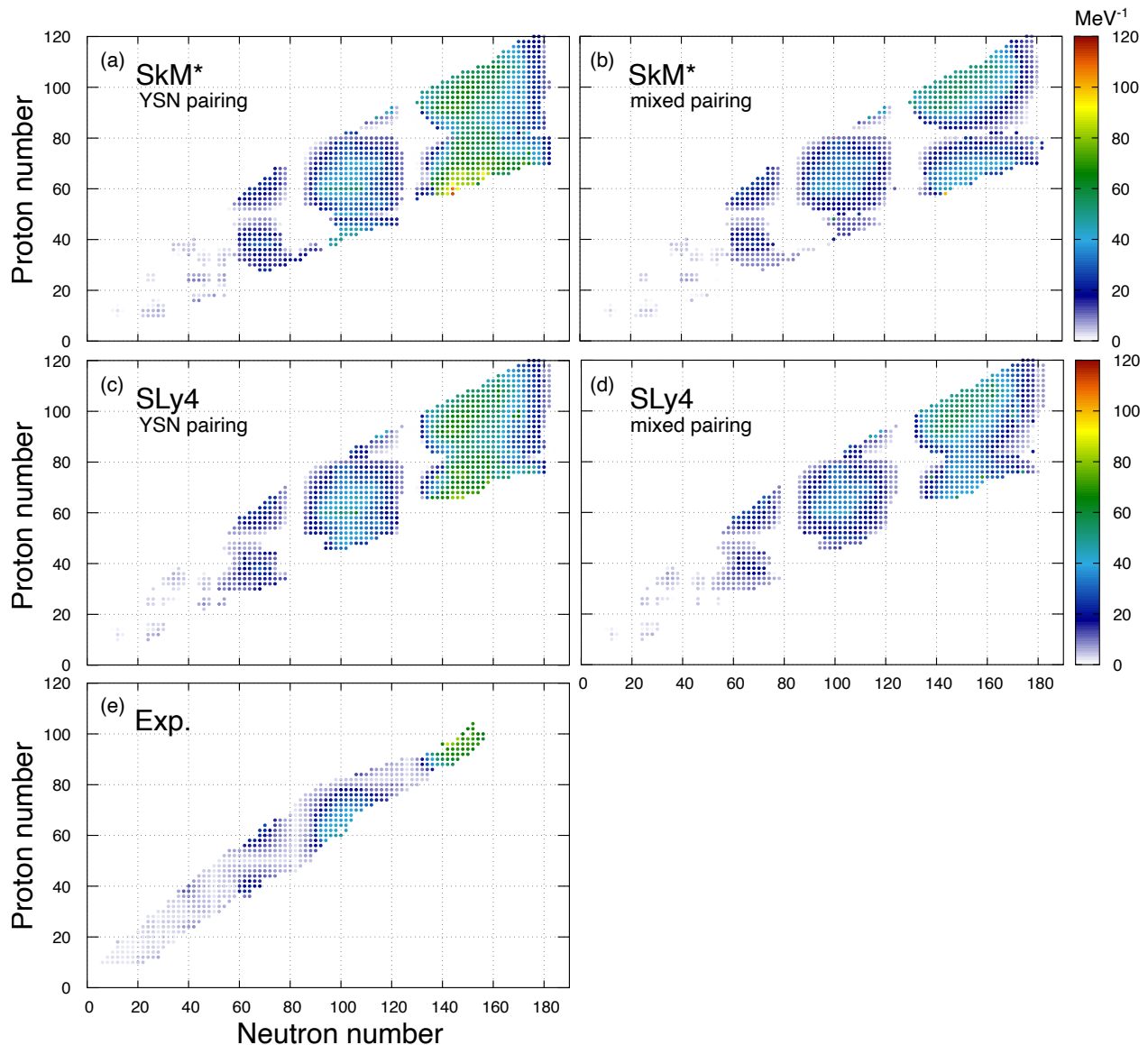


FIG. 1. Calculated moments of inertia \mathcal{J} for the SkM* and SLy4 functionals. The experimental data are taken from Ref. [39], which is evaluated as $3/E(2_1^+)$.

formation; see Fig.1 of Ref. [42]. There are 396 even-even nuclei with known β [39], where the deformation parameter is evaluated from the $E2$ transition probability: $\beta = (4\pi/3ZR_0^2)\sqrt{B(E2)}/e^2$ [14]. I exclude 10 very light nuclei ($Z < 10$). An additional 156 (146) spherical nuclei have been eliminated as in the above analysis, leaving 230 (240) nuclei. I define the measure $R_\beta = \ln(\beta_{\text{cal}}/\beta_{\text{exp}})$ similarly to $E(2_1^+)$. I then find $\bar{R}_\beta = -0.12(-0.11)$ with the dispersion $\sigma = 0.12(0.09)$ for SkM* (SLy4), and $\bar{R}_\beta = -0.08(-0.09)$, $\sigma = 0.07(0.05)$ for 219 (233) nuclei with $\beta > 0.1$. The performance is as good as for the MoI.

B. Moments of inertia of drip-line nuclei

Then, I investigate the MoI of neutron-rich nuclei, and discuss unique features near the drip line. Figures 1(a) and 1(c) show the calculated MoI. I include the even-even nuclei up to $Z = 120$ and below the magic number of $N = 184$. A striking feature observed in the result shown in Fig. 1 is that the deformation is strong in the neutron-rich lanthanide nuclei around $N = 100$ and that the MoI are large accordingly. Furthermore, the MoI of the rare-earth nuclei near the drip line are comparable to those of the heavy actinide nuclei, although the mass number is different by about 40.

I take neutron-rich Dy isotopes as an example of rare-earth nuclei, and investigate in detail the mechanism of

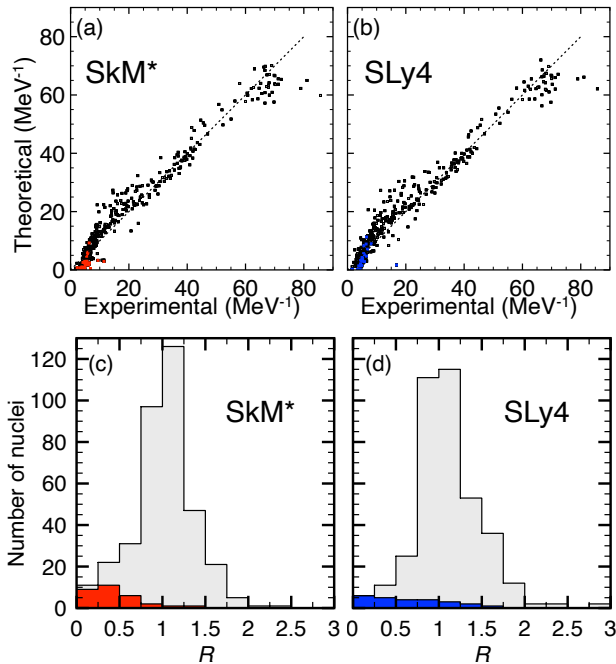


FIG. 2. Calculated MoI for 362 nuclei for the SkM* functional (a) and 375 nuclei for the SLy4 functional (b), plotted versus experimental ones. Filled symbols indicate 30 (25) nuclei possessing a weak deformation with $\beta < 0.1$ with SkM* (SLy4). Histogram of the quantity $R = \mathcal{J}_{\text{th}}/\mathcal{J}_{\text{exp}}$ for the SkM* (c) and SLy4 (d) data set. The area in dark indicates nuclei possessing a weak deformation with $\beta < 0.1$.

TABLE I. Statistics for the performance of the CHFB calculations. Averages \bar{R}_E and standard deviations σ_E for measured $E(2^+)$ are summarized. The values for MAP and GCM are taken from Ref. [40], while 5DCH from Ref. [41].

model	# of nuclei	\bar{R}_E	σ_E
CHFB (SkM*+YSN)	332	-0.021	0.11
CHFB (SkM*+mixed)	325	0.029	0.12
CHFB (SLy4+YSN)	350	-0.095	0.09
CHFB (SLy4+mixed)	356	-0.053	0.14
MAP (SLy4)	359	0.28	0.49
MAP (SLy4, deformed)	135	0.20	0.30
GCM (SLy4)	359	0.51	0.38
GCM (SLy4, deformed)	135	0.27	0.33
5DCH (D1S)	519	0.12	0.33
5DCH (D1S, deformed)	146	-0.05	0.19

the enhanced MoI near the drip line. Figure 3 shows the calculated MoI together with the deformation parameters for $N = 90-120$ and $N = 140-160$. These isotopes are well deformed $\beta \gtrsim 0.2$ and the estimation of $E(2^+)$ is reliable. The experimental data for β are available up to $N = 98$, and the present calculation well reproduces the isotopic dependence. The $E(2^+)$ value is measured up to $N = 106$ [43]. Despite the largest deformation being expected at $N = 100$, the MoI is the largest at $N = 98$ and 104. The calculation also produces the largest

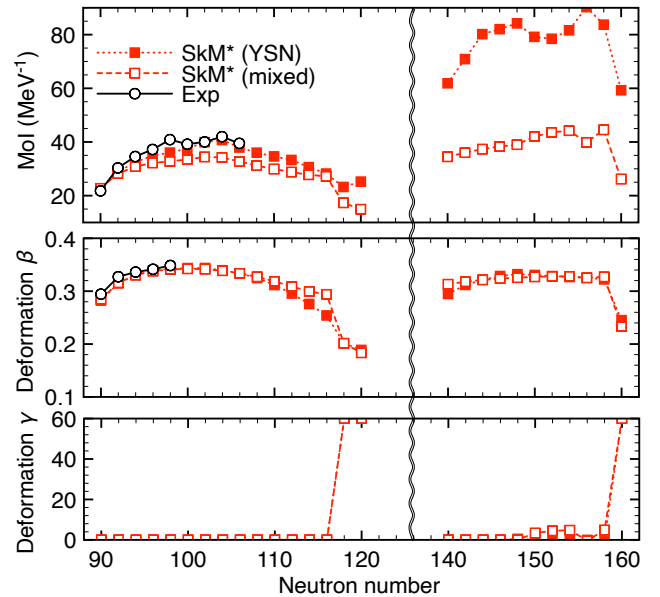


FIG. 3. (Upper) MoI for the Dy isotopes with $N = 90-120$ and $N = 140-160$. (Middle) Deformation parameters β of protons. (Lower) Deformation parameters γ (in degree) of protons. Calculated values are compared with available experimental data [39]. The experimental data for $N = 106$ are taken from Ref. [43].

MoI at $N = 104$. This is due to the weakening of the pairing of neutrons: The pairing gap energy of neutrons is the lowest at $N = 104$ among the isotopes with $N = 90-112$. The increase at $N = 120$ is due to the vanishing pairing gap of neutrons. The value of MoI is sensitively determined by the shell effect and the pairing rather than the magnitude of deformation.

An exotic behavior shows up when approaching the drip line. The MoI in the isotopes with $N \sim 150$ is about twice as large as that in the $N \sim 100$ region, although the deformation of protons is almost the same. Since the neutrons are spatially extended, β of neutrons and of matter are both smaller than those in the $N \sim 100$ region, which is against a naïve perspective for large MoI. The pairing is a possible origin of this unique feature near the drip line.

In asymmetric systems, the isovector densities appear to play a role. To see the effects of the isovector densities in the pairing density functional, I perform the calculation without the ρ_1 terms in Eq. (2); the parameters η_1, η_2 are set to zero while keeping $\eta_0 = 1/2$. This corresponds to the mixed volume and surface. The strength V_0 in Eq. (1) was fixed to the pairing gaps of ^{156}Dy for the YSN functional [36]. I found the strength $V_0 = -289$ (-326) MeV fm³ and -324 (-343) MeV fm³ for neutrons and protons with SkM* (SLy4) produces the same pairing gaps to the ones obtained using the YSN functional. The performance for describing $E(2^+)$ is as good as the YSN functional, as listed in Table I. The calculated MoI are displayed in Figs. 1(b) and 1(d).

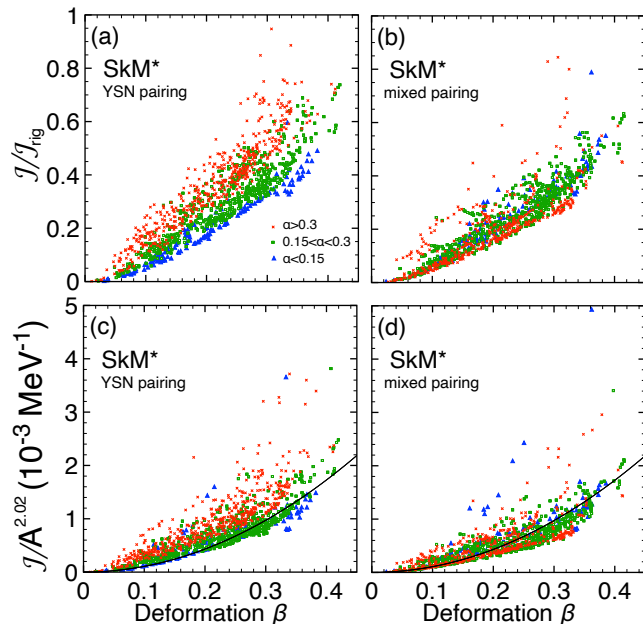


FIG. 4. Ratio of the MoI calculated by using the YSN (a) and mixed-type (b) pairing functional and the ones for the rigid body. The calculated MoI divided by $A^{2.02}$ as a function of the deformation parameter β using the YSN (c) and mixed-type (d) pairing. The line represents Eq. (4) with the approximation $R_0 = 1.2A^{1/3}$ fm. Symbols with cross, square, and triangle indicate the asymmetry parameter $\alpha \geq 0.3$, $0.15 \leq \alpha < 0.3$, and $\alpha < 0.15$, respectively.

The results for the neutron-rich Dy isotopes are shown in Fig. 3. The magnitude of deformation is similar to that calculated with the YSN functional for both in the $N \sim 100$ and $N \sim 150$ regions. The calculated MoI are slightly smaller around $N = 100$, and a 16% reduction is found at $N = 104$. A deformed-shell effect sensitively affects the MoI when using the YSN functional. With the mixed-type pairing, the pairing gap of neutrons decreases gradually from $N = 90$ to 114. Near the drip line, the mixed-type pairing gives almost 50% reduction of MoI to the YSN pairing.

A significant enhancement of MoI near the drip line using the YSN functional is due to a deformed-shell effect and an isovector-density dependence (an effective decrease in the strength) of the pairing functional. Indeed, this mechanism explains the lowering of $E(2_1^+)$ in ^{40}Mg [29]. The reduction in the strength of the pair interaction with an increase in the asymmetry can be seen by the comparison of Figs. 4(a) and 4(b). A reduction of the MoI relative to the rigid body is due to the pairing, and the reduction found in very neutron-rich nuclei with the asymmetry $\alpha = (N - Z)/A > 0.3$ is apparently weakened when using the YSN pairing functional. Scattering of the data points is associated with the shell effect.

Finally, I discuss the enhancement of MoI in a different point of view. As the quadrupole collectivity increases, one sees a lower energy and a stronger transition. Empir-

ically, the following relation has been found and the 91% of the observed 328 data points are reproduced within a factor of two [44]:

$$\left[\frac{B(E2; 0_1^+ \rightarrow 2_1^+)}{1 e^2 \text{fm}^4} \right] \times \left[\frac{E(2_1^+)}{1 \text{MeV}} \right] = 32.6 \frac{Z^2}{A^{0.69}}. \quad (3)$$

This corresponds to

$$\mathcal{J} = \frac{3}{32.6} \left(\frac{3}{4\pi} \right)^2 A^{0.69} R_0^4 \beta^2 [\text{MeV}^{-1}], \quad (4)$$

where R_0 is given in the unit of fm. Figures 4(c) and 4(d) show the calculated MoI divided by $A^{2.02}$ as a function of the deformation parameter β . With the mixed-type pairing, the calculated MoI scatter around the empirical line, and most of them are within a factor of two. On the other hand, with the YSN functional, the empirical line is entirely off the trend of the calculated MoI for $\alpha > 0.3$. Therefore, $E(2_1^+)$ can be low in neutron-rich nuclei despite the $B(E2)$ value is not high. A systematic measurement of $E(2_1^+)$ and $B(E2)$ in neutron-rich nuclei deepens the understanding of the pairing in nuclei and puts a constraint on the pairing density functional.

IV. SUMMARY

I have performed systematic calculations of the MoI from the proton drip line to the neutron drip line to see the roles of neutron excess in the collective rotational motion. To describe neutron-rich nuclei where the loosely-bound neutrons and the continuum coupling are necessary to consider, the cranked HFB equation is solved in the coordinate space. The comparison with the available experimental data and other models shows that the present model surprisingly well describes the ground-state MoI, namely the $E(2_1^+)$ value, for deformed nuclei with $\beta > 0.1$. By employing the pairing density functional constructed to describe the isospin dependence in neutron-rich nuclei, I have found that the MoI are greatly enhanced near the drip line, whereas the magnitude of deformation is not as strong as estimated by the empirical relation between the $E(2_1^+)$ and $B(E2)$ values. A systematic measurement of $E(2_1^+)$ and $B(E2)$ in neutron-rich nuclei puts a constraint on the density dependence of the pairing effective interaction. The stronger the isovector-density dependence is, the more significant the enhancement of MoI in neutron-rich nuclei is.

ACKNOWLEDGMENTS

This work was supported by the JSPS KAKENHI (Grants No. JP19K03824 and No. JP19K03872). The numerical calculations were performed on the computing facilities at the Yukawa Institute for Theoretical Physics, Kyoto University, at the Research Center for Nuclear Physics, Osaka University, and at the Cybermedia Center, Osaka University.

-
- [1] A. Bohr and B. Mottelson, *Nuclear Structure: Volume II, Nuclear Deformations* (Benjamin, Reading, MA, 1975).
- [2] Shell Evolution And Search for Two-plus energies At RIBF: SEASTAR project , <https://www.nishina.riken.jp/collaboration/SUNFLOWER/experiment/seastar/index.php>.
- [3] A. Gade, Excitation energies in neutron-rich rare isotopes as indicators of changing shell structure, *Eur. Phys. J. A* **51**, 118 (2015).
- [4] T. Otsuka, A. Gade, O. Sorlin, T. Suzuki, and Y. Utsuno, Evolution of shell structure in exotic nuclei, *Rev. Mod. Phys.* **92**, 015002 (2020).
- [5] H. L. Crawford, P. Fallon, A. O. Macchiavelli, P. Doornenbal, N. Aoi, F. Browne, C. M. Campbell, S. Chen, R. M. Clark, M. L. Cortés, M. Cromaz, E. Ideguchi, M. D. Jones, R. Kanungo, M. MacCormick, S. Momiyama, I. Murray, M. Niikura, S. Paschalis, M. Petri, H. Sakurai, M. Salathe, P. Schrock, D. Steppenbeck, S. Takeuchi, Y. K. Tanaka, R. Taniuchi, H. Wang, and K. Wimmer, First Spectroscopy of the Near Drip-line Nucleus ^{40}Mg , *Phys. Rev. Lett.* **122**, 052501 (2019).
- [6] J. Terasaki, H. Flocard, P.-H. Heenen, and P. Bonche, Deformation of nuclei close to the two-neutron drip line in the Mg region, *Nucl. Phys. A* **621**, 706 (1997).
- [7] R. Rodríguez-Guzmán, J. Egido, and L. Robledo, Correlations beyond the mean field in magnesium isotopes: angular momentum projection and configuration mixing, *Nucl. Phys. A* **709**, 201 (2002).
- [8] K. Yoshida, Skyrme-QRPA calculations for low-lying excitation modes in deformed neutron-rich nuclei, *Eur. Phys. J. A* **42**, 583 (2009), [arXiv:0902.3053 \[nucl-th\]](https://arxiv.org/abs/0902.3053).
- [9] K. Yoshida, Collective modes of excitation in deformed neutron-rich Mg isotopes, *Mod. Phys. Lett. A* **25**, 1783 (2010).
- [10] J. M. Yao, H. Mei, H. Chen, J. Meng, P. Ring, and D. Vretenar, Configuration mixing of angular-momentum projected triaxial relativistic mean-field wave functions. II. Microscopic analysis of low-lying states in magnesium isotopes, *Phys. Rev. C* **83**, 014308 (2011), [arXiv:1006.1400 \[nucl-th\]](https://arxiv.org/abs/1006.1400).
- [11] S. Watanabe, K. Minomo, M. Shimada, S. Tagami, M. Kimura, M. Takechi, M. Fukuda, D. Nishimura, T. Suzuki, T. Matsumoto, Y. R. Shimizu, and M. Yahiro, Ground-state properties of neutron-rich Mg isotopes, *Phys. Rev. C* **89**, 044610 (2014), [arXiv:1404.2373 \[nucl-th\]](https://arxiv.org/abs/1404.2373).
- [12] T. R. Rodríguez, Precise description of nuclear spectra with Gogny energy density functional methods, *Eur. Phys. J. A* **52**, 190 (2016).
- [13] M. Shimada, S. Watanabe, S. Tagami, T. Matsumoto, Y. R. Shimizu, and M. Yahiro, Simultaneous analysis of matter radii, transition probabilities, and excitation energies of Mg isotopes by angular-momentum-projected configuration-mixing calculations, *Phys. Rev. C* **93**, 064314 (2016), [arXiv:1605.08585 \[nucl-th\]](https://arxiv.org/abs/1605.08585).
- [14] P. Ring and P. Schuck, *The nuclear many-body problem* (Springer-Verlag, New York, 1980).
- [15] D. M. Brink and R. A. Broglia, *Nuclear Superfluidity: Pairing in Finite Systems*, Cambridge Monographs on Particle Physics, Nuclear Physics and Cosmology (Cambridge University Press, 2005).
- [16] K. Matsuyanagi, N. Hinohara, and K. Sato, BCS-Pairing and Nuclear Vibrations, *Fifty Years of Nuclear BCS* , **111–124** (2013), [arXiv:1205.0078 \[nucl-th\]](https://arxiv.org/abs/1205.0078).
- [17] A. Bulgac, Hartree-Fock-Bogolyubov approximation for finite systems, (1980), [arXiv:nucl-th/9907088](https://arxiv.org/abs/nucl-th/9907088).
- [18] J. Dobaczewski, H. Flocard, and J. Treiner, Hartree-Fock-Bogolyubov description of nuclei near the neutron-drip line, *Nucl. Phys. A* **422**, 103 (1984).
- [19] E. Terán, V. E. Oberacker, and A. S. Umar, Axially symmetric Hartree-Fock-Bogoliubov calculations for nuclei near the drip lines, *Phys. Rev. C* **67**, 064314 (2003).
- [20] A. Blazkiewicz, V. E. Oberacker, A. S. Umar, and M. Stoitsov, Coordinate space Hartree-Fock-Bogoliubov calculations for the zirconium isotope chain up to the two-neutron drip line, *Phys. Rev. C* **71**, 054321 (2005).
- [21] K. Yoshida and N. Van Giai, Low-lying dipole resonance in neutron-rich Ne isotopes, *Phys. Rev. C* **78**, 014305 (2008).
- [22] H. Oba and M. Matsuo, Deformation around Neutron-Rich Cr Isotopes in Axially Symmetric Skyrme-Hartree-Fock-Bogoliubov Method, *Prog. Theor. Phys.* **120**, 143 (2008), <https://academic.oup.com/ptp/article-pdf/120/1/143/19572180/120-1-143.pdf>.
- [23] J. C. Pei, M. V. Stoitsov, G. I. Fann, W. Nazarewicz, N. Schunck, and F. R. Xu, Deformed coordinate-space Hartree-Fock-Bogoliubov approach to weakly bound nuclei and large deformations, *Phys. Rev. C* **78**, 064306 (2008).
- [24] H. Kasuya and K. Yoshida, Hartree-Fock-Bogoliubov theory for odd-mass nuclei with a time-odd constraint and application to deformed halo nuclei, *PTEP* **2021**, 013D01 (2021), [arXiv:2005.03276 \[nucl-th\]](https://arxiv.org/abs/2005.03276).
- [25] J. Terasaki, P.-H. Heenen, H. Flocard, and P. Bonche, 3D solution of Hartree-Fock-Bogoliubov equations for drip-line nuclei, *Nuclear Physics A* **600**, 371 (1996).
- [26] S. Jin, A. Bulgac, K. Roche, and G. Wlazlowski, Coordinate-space solver for superfluid many-fermion systems with the shifted conjugate-orthogonal conjugate-gradient method, *Phys. Rev. C* **95**, 044302 (2017), [arXiv:1608.03711 \[nucl-th\]](https://arxiv.org/abs/1608.03711).
- [27] Y. Kashiwaba and T. Nakatsukasa, Coordinate-space solver for finite-temperature Hartree-Fock-Bogoliubov calculations using the shifted Krylov method, *Phys. Rev. C* **101**, 045804 (2020), [arXiv:2001.00500 \[nucl-th\]](https://arxiv.org/abs/2001.00500).
- [28] A. V. Afanasjev, N. Itagaki, and D. Ray, Rotational excitations in near neutron-drip line nuclei: The birth and death of particle-bound rotational bands and the extension of nuclear landscape beyond spin zero neutron drip line, *Phys. Lett. B* **794**, 7 (2019), [arXiv:1905.11500 \[nucl-th\]](https://arxiv.org/abs/1905.11500).
- [29] K. Yoshida, Cranked Skyrme-Hartree-Fock-Bogoliubov approach for a mean-field description of nuclear rotations near the drip line, *Phys. Rev. C* **105**, 024313 (2022), [arXiv:2109.08328 \[nucl-th\]](https://arxiv.org/abs/2109.08328).
- [30] P. Bonche, H. Flocard, and P. Heenen, Self-consistent calculation of nuclear rotations: The complete yrast line of ^{24}Mg , *Nucl. Phys. A* **467**, 115 (1987).
- [31] H. Ogasawara, K. Yoshida, M. Yamagami, S. Mizutori, and K. Matsuyanagi, Rotational Frequency Dependence of Octupole Vibrations on Superdeformed States in ^{40}Ca , *Prog. Theor. Phys.* **121**, 357 (2009).

- [32] ScaLAPACK—Scalable Linear Algebra PACKage, <http://www.netlib.org/scalapack/>.
- [33] A. Baran, A. Bulgac, M. M. Forbes, G. Hagen, W. Nazarewicz, N. Schunck, and M. V. Stoitsov, Broyden’s method in nuclear structure calculations, *Phys. Rev. C* **78**, 014318 (2008).
- [34] J. Bartel, P. Quentin, M. Brack, C. Guet, and H.-B. Håkansson, Towards a better parametrisation of Skyrme-like effective forces: A critical study of the SkM force, *Nucl. Phys. A* **386**, 79 (1982).
- [35] E. Chabanat, P. Bonche, P. Haensel, J. Meyer, and R. Schaeffer, A Skyrme parametrization from subnuclear to neutron star densities. 2. Nuclei far from stabilities, *Nucl. Phys. A* **635**, 231 (1998), [Erratum: *Nucl. Phys. A* 643, 441–441 (1998)].
- [36] M. Yamagami, Y. R. Shimizu, and T. Nakatsukasa, Optimal pair density functional for description of nuclei with large neutron excess, *Phys. Rev. C* **80**, 064301 (2009), [arXiv:0812.3197 \[nucl-th\]](https://arxiv.org/abs/0812.3197).
- [37] J. Margueron, H. Sagawa, and K. Hagino, BCS-BEC crossover of neutron pairs in symmetric and asymmetric nuclear matters, *Phys. Rev. C* **76**, 064316 (2007), [arXiv:0710.4241 \[nucl-th\]](https://arxiv.org/abs/0710.4241).
- [38] J. Margueron, H. Sagawa, and K. Hagino, Effective pairing interactions with isospin density dependence, *Phys. Rev. C* **77**, 054309 (2008), [arXiv:0712.3644 \[nucl-th\]](https://arxiv.org/abs/0712.3644).
- [39] National Nuclear Data Center, “Evaluated Nuclear Structure Data File”, <https://www.nndc.bnl.gov/ensdf/>.
- [40] B. Sabbey, M. Bender, G. F. Bertsch, and P.-H. Heenen, Global study of the spectroscopic properties of the first 2^+ state in even-even nuclei, *Phys. Rev. C* **75**, 044305 (2007).
- [41] G. F. Bertsch, M. Girod, S. Hilaire, J.-P. Delaroche, H. Goutte, and S. Péru, Systematics of the First 2^+ Excitation with the Gogny Interaction, *Phys. Rev. Lett.* **99**, 032502 (2007).
- [42] K. Yoshida and T. Nakatsukasa, Dipole responses in Nd and Sm isotopes with shape transitions, *Phys. Rev. C* **83**, 021304 (2011), [arXiv:1008.1520 \[nucl-th\]](https://arxiv.org/abs/1008.1520).
- [43] H. Watanabe *et al.*, Long-lived K isomer and enhanced γ vibration in the neutron-rich nucleus ^{172}Dy : Collectivity beyond double midshell, *Phys. Lett. B* **760**, 641 (2016).
- [44] S. Raman, C. Nestor, and P. Tikkanen, Transition probability from the ground to the first-excited 2^+ state of even-even nuclides, *At. Data Nucl. Data Tables* **78**, 1 (2001).